Journal of Theoretical and Applied Mechanics, Sofia, 2011, vol. 41, No. 3, pp. 19–30

SOLID MECHANICS

MAXIMUMS AND LOCATIONS OF NORMAL SHEAR STRESSES IN RAILWAY RAIL-WHEEL CONTACT*

N. Nikolov
Institute of Mechanics, Bulgarian Academy of Sciences,
Acad. G. Bonchev St., Bl. 4, 1113 Sofia, Bulgaria,
e-mail: n.nikolov@imbm.bas.bg

T. Avdjieva
Faculty of Physics, University of Sofia "St Kliment Ohridski",
5, J. Bourchier St., 1164 Sofia, Bulgaria,
e-mail: tavdjieva@phys.uni-sofia.bg

[Received 06 October 2011. Accepted 14 November 2011]

Abstract. Contact "rail–wheel" under static load 12 tons is numerically investigated applying design of experiments. The maximal normal and shear stresses and their co-ordinates are mathematically modelled depending on ratios of elastic modules and yield strengths of rail and wheel.

Significant influence of rail yield strength is established. Low rail yield strengths than 630MPa shift the maximal normal pressure stress from the loading centre and provoke low shear stresses in large material volumes possessing maximums located in depth 4 mm and distance 12–15 mm. High rail yield strengths than 630 MPa concentrate high shear stresses in small material volumes with maximums located close to the rail surface in depth 1.8 mm and distance 6 mm each from one other.

The proposed models and diagrams permit easy estimating the contact effects caused by mechanical characteristics; analyzing and predicting micro-crack behaviour; realizing optimal contact by properly chosen mechanical characteristics of both the rail and wheel materials.

Key words: railway steel; elasticity; plasticity; normal and shear stresses; finite element analysis

*Corresponding author e-mail: n.nikolov@imbm.bas.bg

1. Introduction

The interactions between the wheel and rail are the physical basis of the movement of train compositions along the railway. Obviously, the railway exploitation time and traffic safety depend on this interaction. It is observed that the cracks do not generate and propagate in regions outer of the contacting [1]. The mechanical properties of rail become an essential governing part in such undesirable damage processes [2, 3], due to this phenomenon. Not rarely, a crack could bring about breaking off a piece of rail in the damaged volumes. The thickness of the so called "squat" type crack, appearing in the rail–wheel contact zone, yields maximal value of 0.1 mm, and the crack volume reaches a value of 115 mm^3 [4]. The cracks may branch to Mode 1 direction when the residual stress, crack inclination and braking force create favourable conditions [5]. In these type of cracks the process of thickness formation and growing is very complicated. The development of crack thickness could be also stimulated by the combined effects of very high contact stresses between the wheel and the rail head, wear process, water penetration into the increasing crack *etc.* Thereby, the investigations on the material properties and internal stresses inside rail sections appear as important tasks in the recent state of the art [6]. Once the stresses has been computed, they can be used then to predict the direction and rate of crack growth through stress intensity factors including full Modes 1–3 computations [7]. The cracks could originate from the rail surface or underneath it, depending on the operating conditions and material [8]. For this reason, the knowledge of stress state in the rail head gained on the basis mathematical modelling is the aim of this elaboration. Such kind data could be a successful contribution in predicting damage and crack behaviour and useful tool in help of designers and producers of railway rails and wheels.

2. Theoretical basis

It is seen from Section 1, the interaction between rails and wheels has been investigated since decades, but independently on that a number of unresolved problems still remain. The object of present study is an aspect of this problem, namely, mathematical modelling the influence of rail and wheel material characteristics, loading and contact types on normal and shear stresses and their locations during the interaction in the contact pair "rail-wheel".

A complex of factors influences the exploitation time of railway rails. The contact-fatigue processes, material plastic deformation, crack behaviour and wear are some of them. The understanding of the mechanism of contact processes could happen only if the interaction between the rail and the wheel is

known during their relative displacement. Not occasionally, the Finite Element Method (FEM) is widely used in order to apply analytical methods during the investigation of contact parameters.

The analysis of normal and shear stress distributions in the rail head, could introduce clarity about the circumstances concerning initiation, growth, arrest, closure and growth of the threshold of cracks and evolution of eventual damages in the rail. The real experiments for establishment the stress distribution are related to design of special equipment and caring out a number of experiments aiming stability of the results. A proper numerical simulation based on the experience avoids the pointed out difficulties and could spearhead the attention in some essential details whose studying experimentally is not so easy. On the other hand, such simulation data could help the planning of real experiments as well as a design of special experimental equipment.

Basically, during the movement of train composition the contact point is not situated along the central line of both elements. Consequently, the conditions in the contact point through the different rail and wheel contacting radii manage the stress-strain state of both the elements in different way. A significant role of the contact parameters in the crack behaviour and contact fatigue processes follows from this fact. The maximal normal, maximal contact and maximal shear stresses possess different values depending on the geometry of contact interactions between the rail and wheel. These circumstances motivate the treatment of one-point contact during the investigations reported in this paper.

3. Finite Element (FE) model of pieces in rail-wheel contact

A case of one-point contact is numerically modelled and investigated applying ANSYS-FEM computer code. The geometrical model of the contact pair is structured introducing parts of standard rail and wheel profiles, presented in Fig 1a, b.

The rail and wheel piece volumes are modelled by 16972 finite elements of types Solid95. Both the rail and wheel piece volumes contain 12489 and 13522 nodes. The 444 contact elements Conta174 overlay the 7736 solid elements describing the boundary of rail and are potentially in contact with 376 target segment elements Targe170 describing the wheel target surface. Both materials are modelled by bilinear models using data presented in Table 1. The actual rail and wheel profile sizes are given in Fig. 1c. The wheel is loaded by 12 tons. Corresponding symmetrical boundary conditions are imposed taking into account the symmetry of rail and wheel in plane XY and symmetry of rail

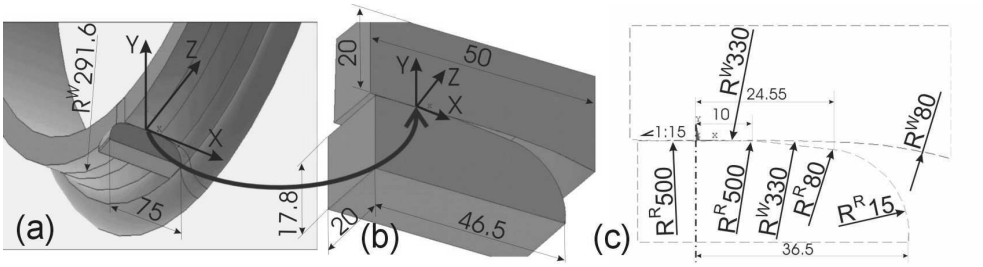

Fig. 1. Finite element model of (a) contact, (b) FE-pieces, (c) sizes

with respect to plane YZ, in Fig. 1b. The wheel rolling along the rail causes variable contacts from a lateral, through one-point to two-point, please refer to Fig. 1a [9]. For this purpose, the centre of contact, in which the centre of co-ordinate system XYZ is embedded, is chosen in the transition point between both the rail radii R^R500 on the left and right sides of axis Y, respectively (Fig. 1c). This point contacts (Fig. 1a) with the transition point between the wheel radius R^W330 protuberant with respect to axis X in right-hand side and slope $\angle 1:15$ on the left. In the case of discussed one-point contact, the highest load on the rail is concentrated in this point. Two-point contact is realizable when the co-ordinate centre XYZ contacts with the transition point between both the protuberant and concave wheel radii R^W330.

4. Full Factorial Design of Experiments

In this elaboration, a numerical procedure with design of experiments is applied because of the complexity of the rail-wheel contact and wide ranges of variance of the mechanical characteristics. The assumed orthogonal centrally-composed design of experiments possesses three significant levels of the ratio of the wheel elastic module to this of the rail and the three significant levels of both the rail and the wheel yield strengths. Ratio $E^{WR} = E^W/E^R$ of the elastic module of wheel E^W to this of the rail E^R is chosen in limits of 0.84–1.19 according to the practice and experimental observations [2, 9].

With $E^W/E^R = 0.84$, and $E^W = 178.08$ GPa, $E^R = 212$ GPa.

With $E^W/E^R = 1.19047$, and $E^W = 212.00$ GPa, $E^R = 178.08$ GPa.

With $E^W/E^R = 1.0152$, and $E^W = 195.04$ GPa $= E^R = 195.04$ GPa.

Variations of yield stress of rail σ_P^R are defined on the range of $\sigma_P^R = 160 - 1100$ MPa. Variations of yield stress of wheel σ_P^W are chosen on the range of $\sigma_P^W = 550 - 850$ MPa. These variation ranges are defined through

Table 1. Design of Experiments; Normal stresses [MPa] and their co-ordinates [mm]

Design of Experiments				Results			
No	E^{Wh}/E^{Rail}	σ_P^{Rail}	σ_P^{Wh}	σ_Y	σ_Y^m	$C_X^{\sigma Y}$	$C_Z^{\sigma Y}$
1	0.84	160	550	−484.5	−482.6	−1.7	−3.7
2	1.19	160	550	−476.3	−474.9	−1.7	−3.7
3	0.84	1100	550	−1287.3	−1290.5	0	0
4	1.19	1100	550	−1276.7	−1277.4	0	0
5	0.84	160	850	−484.5	−483.9	−1.7	−3.7
6	1.19	160	850	−476.3	−473.2	−1.7	−3.7
7	0.84	1100	850	−1317.1	−1318.6	0	0
8	1.19	1100	850	−1300.5	−1302.4	0	0
9	1.19	630	700	−1174.2	−1176.3	0	0
10	0.84	630	700	−1190.4	−1188.3	0	0
11	1.01	1100	700	−1313.6	−1306.4	0	0
12	1.01	160	700	−480.54	−487.82	−1.7	−3.7
13	1.01	630	850	−1184.6	−1185.1	0	0
14	1.01	630	550	−1172.5	−1172.2	0	0

real physical experiments at tension of rail steel UIC60 hardened at 840 °C in water and oil and subsequently tempered at intervals 180–550 °C [2, 9]. The different combinations of these material characteristics lead to different conditions of generation, evolution, standing and disappearing micro-cracks or growth to critical sizes.

5. Mathematical models of maximal normal and shear stresses in the rail head

In the mathematical models (1)–(6) reported in this paper, E^{WR}, σ_P^R, σ_P^W are transformed using the dependencies: $E_{WR} = (E^{WR} - 1.01)/0.175$; $\sigma_{PR} = (\sigma_P^R - 630)/470$ and $\sigma_{PW} = (\sigma_P^W - 700)/150$.

The mathematical models of the maximal normal (1) and minimal (2)

and maximal (3) shear stresses possess the types:

$$(1)\quad \sigma_Y = -1185 + 5.97E_{WR} - 409.3\sigma_{PR} - 6.57\sigma_{PW} + 1.35E_{WR}\sigma_{PR} + 0.74E_{WR}\sigma_{PW} - 6.7\sigma_{PR}\sigma_{PW} + 2.7E_{WR}^2 + 287.9\sigma_{PR}^2 + 6.45\sigma_{PW}^2,$$

$$(2)\quad -\tau_{XY} = -257.65 + 0.825E_{WR} - 95.3\sigma_{PR} - 2.48\sigma_{PW} + 0.978E_{WR}\sigma_{PR} + 0.29E_{WR}\sigma_{PW} - 2.798\sigma_{PR}\sigma_{PW} + 1.184E_{WR}^2 + 77.7\sigma_{PR}^2 + 1.56\sigma_{PW}^2,$$

$$(3)\quad +\tau_{XY} = 262.4 - 0.55E_{WR} + 96\sigma_{PR} + 3.64\sigma_{PW} - 0.5E_{WR}\sigma_{PR} - 0.28E_{WR}\sigma_{PW} + 3.15\sigma_{PR}\sigma_{PW} - 0.18E_{WR}^2 - 77.7\sigma_{PR}^2 - 1.8\sigma_{PW}^2,$$

where E_{WR} is the transformed ratio E^{WR} in the interval $[-1;+1]$, σ_{PR} and σ_{PW} are dimensionless rail and wheel yield strengths also in the interval $[-1;+1]$.

The adequacy of mathematical models is checked according to the correlation coefficient R and the corresponding Fisher's criterion F [10]. The values of R are obtained through the scatterings of corresponded output model values given in Tables 1 and 2, about their average values, because additional experiments aiming repetition of results are not performed. The obtained results are for:

— normal pressure stress σ_Y: $R^{\sigma Y} = 0.9999627$, $F^{\sigma Y} = 7456.124$;

— shear stress $\pm\tau_{XY}$: $R^{\tau XY} = 0.9996212$, $F^{\tau XY} = 23898.75$.

The admissible values F_R for the normal stress and the shear stresses are: $F_R^{\sigma_Y,\tau_{XY}}(\alpha,\nu_1,\nu_2) = F_R^{\sigma_Y,\tau_{XY}}(0.05,9,4) = 5.975$, where α, is a given level of significance, $\nu_1 = k-1 = 9$, $\nu_2 = N-k = 4$ are degrees of freedom, and $N = 14$ is the number of experiments, $k = 10$ is the number of coefficients in the models. Since the requirement $F^{\sigma_Y,\tau_{XY}} > F_{R,\nu_1,\nu_2}^{\sigma_Y,\tau_{XY}} = 5.975$ is satisfied, the correlation coefficients R are significant and the conclusions may be drawn that the proposed models are adequate, could be used for predicting, and qualitative analyses performed on their basis could be sufficiently reliable in the practice.

6. Mathematical models of the location of maximal stresses in the rail head

The mathematical models of the location of maximal normal pressure stress in plane XZ in meters have the type:

$$(4a)\qquad C_X^{\sigma Y} = 0.0008493\sigma_{PR} - 0.0008493\sigma_{PR}^2,$$

Table 2. Shear stresses [MPa] and their co-ordinates [mm]

No	$-\tau_{XY}$	$-\tau_{XY}^{m}$	$C_X^{-\tau XY}$	$C_Y^{-\tau XY}$	$+\tau_{XY}$	$+\tau_{XY}^{m}$	$C_X^{+\tau XY}$	$C_Y^{+\tau XY}$
1	−82.3	−81.72	−6.18	−4.08	86.93	89.6	7.838	−4.157
2	−82.5	−82.61	−6.18	−4.08	87.26	90.1	7.838	−4.157
3	−267.6	−268.7	−2.99	−1.83	272.4	276.4	4.947	−1.913
4	−265.0	−265.6	−2.99	−1.83	271.8	274.9	4.947	−1.913
5	−82.3	−81.67	−6.18	−4.08	86.93	87.5	7.838	−4.157
6	−82.59	−81.39	−6.18	−4.08	87.26	86.8	7.838	−4.157
7	−279.9	−279.8	−2.99	−1.83	286.1	286.9	4.947	−1.913
8	−275.0	−275.6	−2.99	−1.83	283.3	284.3	4.947	−1.913
9	−255.8	−255.6	−4.66	−2.15	260.8	261.7	4.947	−1.913
10	−257.1	−257.2	−4.66	−2.15	263.7	262.8	4.947	−1.913
11	−277.4	−275.2	−2.99	−1.83	282.4	280.8	4.947	−1.913
12	−82.4	−84.65	−6.18	−4.08	87.09	88.7	7.838	−4.157
13	−257.3	−258.5	−4.06	−2.15	266.2	264.2	4.947	−1.913
14	−254.9	−253.6	−4.06	−2.15	255.0	260.6	4.947	−1.913

$$C_Z^{\sigma Y} = 0.0018561\sigma_{PR} - 0.0018561\sigma_{PR}^2. \tag{4b}$$

The mathematical models of the location of maximal positive $+\tau_{XY}$ and maximal negative $-\tau_{XY}$ shear stresses in meters have the type:

$$C_X^{-\tau XY} = -0.004066205 + 0.001593950\sigma_{PR} - 0.0005178524\sigma_{PR}^2, \tag{5a}$$

$$C_Y^{-\tau XY} = -0.002151601 + 0.001124950\sigma_{PR} - 0.000809649\sigma_{PR}^2, \tag{5b}$$

$$C_X^{+\tau XY} = 0.004947993 - 0.00144510\sigma_{PR} + 0.001445104\sigma_{PR}^2, \tag{6a}$$

$$C_Y^{+\tau XY} = -0.001913702 + 0.00112185\sigma_{PR} - 0.001121850\sigma_{PR}^2. \tag{6b}$$

7. Analysis of the stress state models

The maximal normal pressure stress σ_Y on the rail is in the interval 470–1300 MPa, and it increases with increasing rail yield strength, Fig. 2a. They are calculated by varying yield stress limit of rail σ_P^R under minimal and maximal values of σ_P^W and E^{WR}. It is seen from models (4) that the location of maximal normal stress on the rail surface, Fig. 2b, depends on the yield stress limit of the rail σ_P^R only. Low rail yield strengths lead to shift of maximal normal pressure stress σ_Y from the loading centre, Fig. 2b.

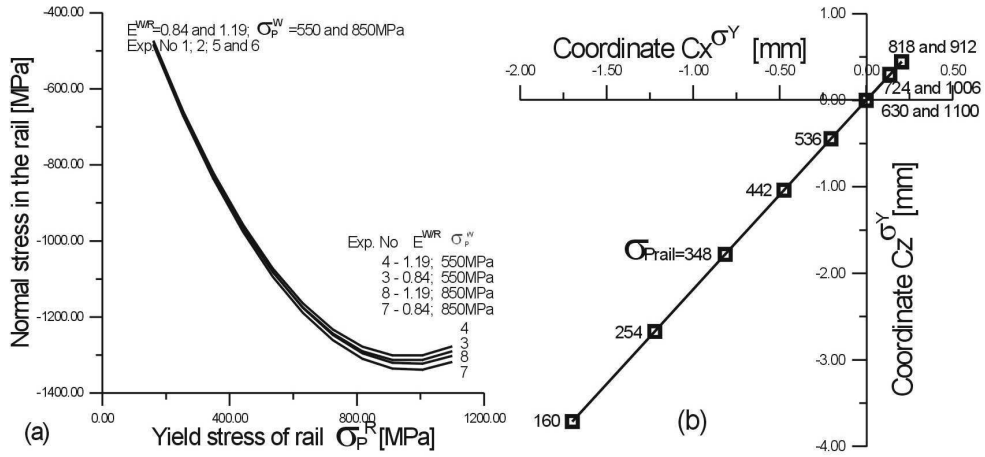

Fig. 2. Normal pressure stress (a) and locations (b) depending on increasing yield stress limit of the rail

In Fig. 3a and b, a comparison between effects caused by the low and the high limit rail strengths in Experiments 6 and 8 is presented.

Low rail yield strength 160 MPa provokes low shear stresses in large material volumes located in depth 4 mm and distance 14 mm, Fig. 3a. High rail yield strength 1100MPa concentrates high shear stresses in small material volumes located close to the rail surface in depth 1.8 mm and distance 8 mm each from one other, Fig. 3b. The simultaneous increase of both yield stress limits causes increasing shear stresses.

The maximal shear stresses τ_{XY} calculated by (2) and (3) are in the interval 80–280 MPa, Fig. 4a, b. From models (5) and (6), it is seen only the rail yield strength influences the depth of maximal shear stresses in the cross-section of the rail head. Moreover, the analysis of (5) and (6) shows that an increase of rail yield strength σ_{PR} causes a decrease of the depths $C_Y^{-\tau XY}$ and $C_Y^{+\tau XY}$ of the absolute maximums of shear stresses $\pm\tau_{XY}$. Depending on

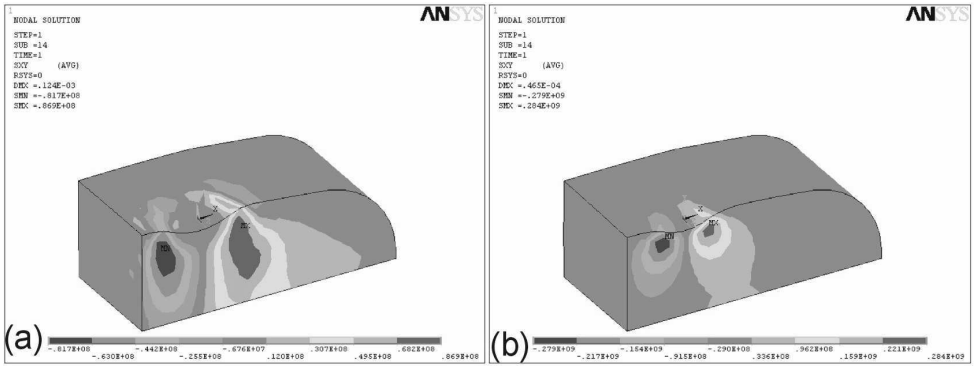

Fig. 3. Shear stress (−) τ_{XY} and (+) τ_{XY} (a) Experiment 6; (b) Experiment 8

σ_{PR}, the different tendencies of the location of absolute shear stress maximums in the cross section of the rail head are seen in the Fig. 4b and c. The higher than 250 MPa absolute values of the positive $+\tau_{XY}$ and the negative shear $-\tau_{XY}$ stresses, caused by high σ_{PR} in order 750–1100 MPa, are concentrated in smaller material volumes (Fig. 3b and 4a, b) and are located closer to the rail surface in depth near to 1.8 mm and in small distance of 6–8 mm each from one other, Fig. 4c, d. The lower than 150 MPa shear stresses τ_{XY} are located in distance 4 mm from the rail surface. The distance between shear stress maximums are in the interval 12–15 mm with lower yield stress limits of rail 160–350 MPa.

8. Conclusions

Parameters of stress state in a pair "railway rail – wagon wheel" (Fig. 1) are mathematically modelled and quantitatively investigated under static load 12 tons depending on mechanical characteristics of both contacting elements. A Full Factorial Design of Experiments (Table 1) is numerically performed. Three significance levels of three mechanical characteristics including the ratio of the elastic module of wheel E^W to this of rail E^W on the range of $E^{WR} = 0.84-1.19$, yield stress limit of the rail on the range of $\sigma_S^R = 160-1100$ MPa, yield stress limit of wheel on the range of $\sigma_S^W = 550-850$ MPa are assumed. The ranges are defined through real physical experiments at tension of rail steel UIC60 hardened and tempered under different conditions [2]. Mathematical models of maximal normal (eq. 1) and maximal shear stresses (eq. 2 and 3) as well as mathematical models of their co-ordinates (eq. 4–6) are derived through Regression analyses.

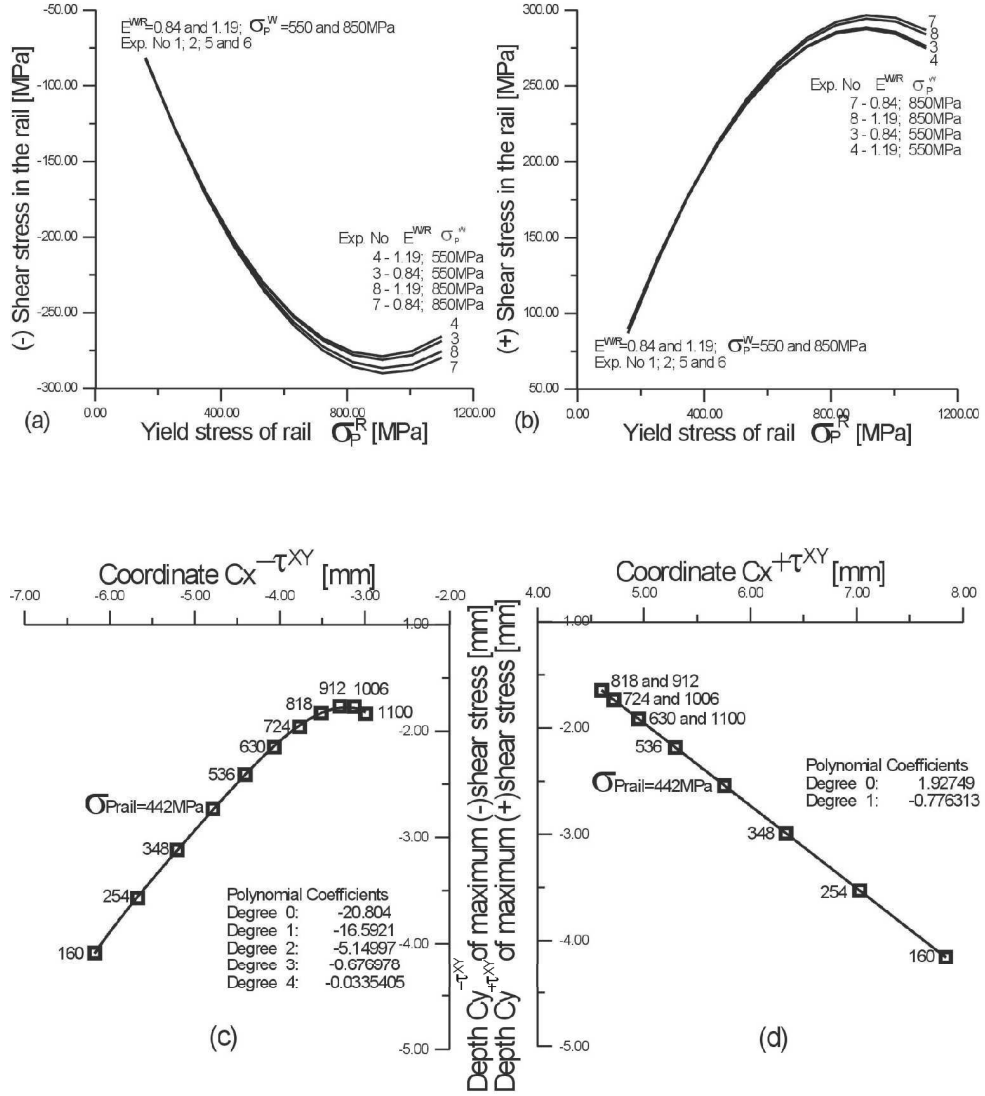

Fig. 4. Maximums of negative (a) and positive (b) shear stresses and their locations (c) and (d) respectively, in the rail cross-section depending on the rail yield stress limit

The maximal normal pressure stress σ_Y on the rail is found in the interval 470–1300 MPa, and it increases with increasing the rail yield strength, Fig. 2a. The maximal shear stresses $(\pm)\tau_{XY}$ are found in the interval 80–280 MPa, Fig. 4a and b. The maximums of normal pressure stresses σ_Y shift from the loading centre, Fig. 2b. The higher absolute values of the positive $(+)\tau_{XY}$ and the negative shear $(-)\tau_{XY}$ stresses are concentrated in smaller material volumes (Fig. 3b) and are located closer to the rail surface in depth 1.8 mm and in smaller distance of 6 mm each from one another, Fig. 4c and d. The lower shear stresses $(\pm)\tau_{XY}$ are located in distance 4 mm from the rail surface, Fig. 3a. The distance between shear stress maximums are in the interval 12–15 mm with lower yield stress limits of rail 160–350 MPa.

The results obtained in this elaboration pose questions about optimal admissible values of maximal stress and significance of their locations in the rail head with respect to the crack behaviour. That could be realized by properly chosen tempering treatments leading to corresponding material structures and mechanical characteristics.

From point of view fracture mechanics, another question arising in this investigation is related to the possibility of predicting the micro-crack behaviour based on the derived models in order to prevent micro-crack initiation and growth.

REFERENCES

[1] Handa, K., Y. Kimura, Y. Mishima. Surface Cracks Initiation on Carbon Steel Railway Wheels under Concurrent Load of Continuous Rolling Contact And Cyclic Frictional Heat. *Wear*, **268** (2010), 50–58.

[2] Avdjieva, T. About The Opportunities To Definite The Elastic Properties Of A Rail Steel Without Using The Specimens, Proc. Xxii Scientific-Expert Conference Railcon'06, Serbia, Nish, 2006, 61–64.

[3] Jiraskova, Y., J. Svoboda, O. Schneeweiss, B. W. Daves, et all. Microscopic Investigation of Surface Layers on Rails. *Appl. Surf. Science*, **239** (2005), 132–141.

[4] Pyrzanowski, P. Estimation and Consequences of the Crack Thickness Parameter in the Assessment of Crack Growth Behaviour of "Squat" Type Cracks in the Rail–Wheel Contact Zone. *Eng. Fract. Mech.*, **74** (2007), 2574–2584.

[5] Bogdanski, S., M. W. Brown. Modelling the Three-Dimensional Behavior of Shallow Rolling Contact Fatigue Cracks in Rails. *Wear*, **253** (2002), 17–25.

[6] Plu, J., S. Bondeux, D. Boulanger, R. Heyder. Application of Fracture Mechanics Methods to Rail Design and Maintenance. *Eng. Fract. Mech.*, **76** (2009), 2602–2611.

[7] Mellings, S., J. Baynham, R. A. Adey. Automatic Crack Growth Prediction in Rails with BEM. *Eng. Fract. Mech.*, **72** (2005), 309–318.

[8] Gerlici, J., T. Lack. Contact Geometry Influence on the Rail/Wheel Surface Stress Distribution, *Proc. Eng.*, No **2** (2010), 2249–2257.

[9] Avdjieva, T., M. Georgiev, N. Nikolov. The influence of Hardness on the Contact Parameters in the Contact Pair "Rail-Wheel", *Proc. International scientifique-technical conference "Advanced technologies and materials"*, Russia, Perm., Nov. 28, 2008, 21–32.

[10] Vuchkov, I., S. Stoyanov. Mathematical Modeling and Optimization of Technological Objects, 1st ed. Sofia, Technics, 1986 (in Bulgarian).